

Research Article

The Study of Properties and Structure of Polylactide–Graphite Nanoplates Compositions

Svetlana Rogovina ¹, **Sergei Lomakin**,^{1,2} **Sergey Usachev**,¹ **Miraga Gasymov**,¹ **Olga Kuznetsova**,¹ **Natalya Shilkina**,¹ **Vitalii Shevchenko**,^{1,3} **Aleksey Shapagin**,⁴ **Eduard Prut**,¹ and **Aleksander Berlin**¹

¹*Semenov Federal Research Center for Chemical Physics, Russian Academy of Sciences, Kosygin St., 4, Moscow 119991, Russia*

²*Emanuel Institute of Biochemical Physics, Russian Academy of Sciences, Kosygin St., 4, Moscow 119991, Russia*

³*Enikolopov Institute of Synthetic Polymeric Materials, Russian Academy of Sciences, Profsoyuznaya St., 70, Moscow 117393, Russia*

⁴*Frumkin Institute of Physical Chemistry and Electrochemistry, Russian Academy of Sciences, Leninsky Av., 31, Bld.4, Moscow 119071, Russia*

Correspondence should be addressed to Svetlana Rogovina; s.rogovina@mail.ru

Received 15 February 2022; Accepted 11 May 2022; Published 31 May 2022

Academic Editor: Meenakshi Gusain

Copyright © 2022 Svetlana Rogovina et al. This is an open access article distributed under the Creative Commons Attribution License, which permits unrestricted use, distribution, and reproduction in any medium, provided the original work is properly cited.

Composites of polylactide containing graphite nanoplates as a filler in the concentration range 1–20 wt% were prepared in methylene chloride using the sonication technique. The thermal characteristics and phase transitions were studied by DSC and TGA methods. The temperatures and heats of glass transition, crystallization, and melting were determined, and the degree of crystallinity during primary and secondary heating was calculated. It is shown that the introduction of graphite nanoplates leads to an increase in the elastic modulus and a decrease in the breaking stress and elongation at break. These changes are especially pronounced at 20% GNP content in the composition, when the corresponding mechanical parameters are characteristics of brittle polymer systems. The study of the electrical properties of the composites showed that the percolation threshold in these materials is close to 7 wt%, which is significantly lower than in the case of spherical particles of comparable density. The SEM study of the filled composites showed a system of pores, which were apparently formed during the evaporation of solvent in the process of their preparation. Diverse structures of PLA/GNP composites films after hot pressure were established by the SEM method.

1. Introduction

The production of polymer compositions based on different types of polymers containing nanosized carbon fillers is currently an actively developing area aimed at creating materials with new properties. The unique peculiarities of two-dimensional carbon compounds provide the materials with their use a whole range of high characteristics, including increased mechanical and thermal stability, as well as an increase in electrical conductivity [1–5].

Polylactide (PLA), synthesized from natural raw materials (lactic acid), belongs to the class of aliphatic polyesters and, due to its physicochemical characteristics, represents an alternative to synthetic polymers [4].

The physical-chemical characteristics of PLA largely depend on its molecular weight and isomeric composition.

Commercially available polylactides are copolymers of poly(L-lactic acid) and poly(D, L-lactic acid), which are derived from L-lactides and D, L-lactides, respectively. The ratio of enantiomers in these polymers affects their crystal structure and properties. Currently, the most common is poly(L-lactic acid), which is a fairly brittle crystalline polymer with good strength and toughness [4].

The tensile and flexural moduli of PLA are higher than those of high-density polyethylene (HDPE), polypropylene, and polystyrene, but the elongation at break is lower compared to these polymers. In general, PLA has the necessary mechanical and barrier properties to compete with the existing

polymer materials. It is well known that aliphatic polyesters, and in particular polylactide, have rather low thermal stability [6–8]. The thermal degradation processes of PLA have been studied in detail previously [7–9]. Thermal degradation of PLA is accompanied by zipper-like depolymerization, intermolecular transesterification with the formation of monomeric and oligomeric esters, as well as by intramolecular transesterification, leading to the formation of oligomers [8]. The formation of specific decomposition products and their ratio depend on such factors as temperature, the presence of additives and impurities in the polymer, as well as the position of the active center in the polylactide chain, which is the beginning of the reaction [8].

The compositions of PLA with various polymers and fillers significantly expand potential areas of its application [9, 10]. Among such different compositions are the thermostable composites of PLA containing nanosized carbon fillers of various types; nanotubes, carbon fibers, graphene, GNP are of special interest, and the search for new areas of their practical use is currently an actively developing field of scientific and applied research [1]. One of the promising carbon nanofiller is thermally expanded graphite, which is formed as a result of thermal action on intercalated graphite compounds. Expanded graphite is a porous structure consisting of graphene layers and is usually used to obtain colloidal solutions of graphene [5, 11].

The use of GNP for the creation of filled compositions based on polylactide is one of prospective directions in this field. Gonçalves et al. analyzed the available information on the mechanical, thermal, electrical, and biological properties, as well as potential applications of PLA composites with carbon nanotubes (CNT) and graphene-based materials (GBM). Both CNT and GBM nanofillers are effective at improving PLA thermomechanical and electrical properties. However, lower amounts of graphene-based materials (0.1–1 wt%) are usually needed when comparing with carbon nanotubes (0.25–5 wt%) [12].

The work of Bortoli et al. described the application of carbon nanotubes to improve the mechanical strength of 3D-printed PLA parts and provide better interfacial adhesion between 3D-printed layers, maintaining the thermal stability of nanocomposites [13].

Lin et al. showed that multiwalled carbon nanotube (MWCNT)/PLA composites exhibit an improvement in conductive property. Such composites made from grafting MWCNT onto polymer chains would be highly efficient for antistatic, electrostatic discharge, or electromagnetic interference EMI shielding purposes and can be applied in electronic materials [14].

In present work, the effect of GNP on the thermal, mechanical, and electrically conductive properties, as well as on the structure of PLA composites containing GNP was studied.

2. Experimental

2.1. Materials. PLA produced by Nature Works (Minnetonka, MN, USA) as pellets with a diameter of 3 mm, $M_w = 2.2 \times 10^5$, $T_m = 155^\circ\text{C}$, and transparency 2.1% and

GNP 5 (XG Sciences, Michigan State University, USA) with diameter $d = 10$ nm, length = 5 μm , relation $L/d = 500$, and density $\rho = 1.8$ g/cm³ were taken as objects of investigation.

In order to obtain PLA film composites containing different amounts of GNP, the pristine PLA was preliminarily dissolved in CH₂Cl₂ at 22°C for 48 hours. The calculated amount of GNP was added to the resulting solution, and the dissolved mixture was sonicated in an ultrasonic bath for 30 min at 10°C. Then, the solvent was removed on a rotary evaporator, and the resulting mixture was dried to constant weight at 55°C for 4 hours. The obtained samples were films on which the subsequent measurements of the thermophysical properties by DSC and TGA methods were carried out.

The PLA and composites PLA/GNP obtained were subjected to hot pressing on a Carver Press (Carver, Inc., Wabash, IN, USA) at 180°C and 10 MPa followed by cooling under the same pressure at a rate of 15°C min⁻¹. As a result, the films of 0.18–0.25 mm were formed. Furthermore, these films were used for mechanical and electrical tests.

2.2. Thermophysical Properties. Thermophysical characteristics and thermal stability of PLA and its compositions with GNP were studied by the differential scanning calorimetry (DSC) method on a DSC-204 F1 (Netzsch, Holding KG, Selb, Germany) calorimeter at the heating rate 10 K/min in inert argon atmosphere and temperature range 25–200°C. The experiments included several consecutive cycles: first heating, cooling, and second heating at the same rate.

Thermogravimetric analysis (TGA) of the samples was performed on the NETZSCH TG 209 F1 Phoenix thermal balance at the heating rate of 20°C/min in inert argon atmosphere under heating rate 20°C/min with flow speed of 40 ml/min. Weight of samples was 6 ± 1 mg.

2.3. Mechanical Properties. Mechanical characteristics of samples were determined on an Instron machine (High Wycombe, UK) under uniaxial stretching at the rate of the upper traverse motion of 50 mm/min at room temperature. From the obtained diagrams, elastic modulus E , tensile strength, and elongation at break were calculated. The results were averaged for five samples.

2.4. Investigation of Electrical Properties. The dielectric properties of nanocomposites (dielectric constant, losses, electrical modulus, and conductivity) were studied in the frequency range from 10⁻¹ to 10⁶ Hz using a Novocontrol Alpha-A impedance analyzer and a ZGS Alpha Active Sample Cell dielectric cell with gold-plated disk electrodes 20 mm in diameter.

2.5. Sample Investigation by the SEM Method. The phase structure of PLA-GNP systems was studied using a Philips SEM-500 scanning electron microscope (the Netherlands) in secondary electrons regime and accelerating voltage of 15 keV. Films and transverse fractures of graphene-modified

polylactide films were used for the analysis. The preparation of the samples consisted in thermal spraying of a thin conductive layer of carbon in the Edwards coating system E306 A (England).

3. Results and Discussion

3.1. Thermophysical Properties of PLA and PLA/GNP Composites. The thermal behavior of initial PLA and in PLA/GNP film composites obtained from CH_2Cl_2 solutions and containing 1, 5, 10, 15, and 20 wt% of GNP was studied using the DSC method. Figures 1 and 2 show typical DSC curves obtained during the first and second heating of PLA and PLA/GNP compositions containing a filler in the range of 1–20 wt%.

The temperatures of glass transition (T_g), cold crystallization (T_{cc}), and melting (T_m) as well as corresponding enthalpies (ΔH_{cc} , ΔH_m) were measured at first and second heating.

As Figure 1 (curve 1) shows, at first heating of the PLA prepared from a methylene chloride solution, only a single endothermic peak of melting at 163.2 °C is observed on the DSC curve in the absence of the cold crystallization effect (Table 1). This fact indicates that already at the stage of PLA film preparation, the organized semicrystalline structure of PLA is formed, which remains unchanged until melting.

At the same time, at first heating of PLA/GNP composites containing 1 and 5 wt% GNP along with endothermic melting peaks of PLA, weakly pronounced peaks of glass transition and cold crystallization are observed (Figure 1, curves 2 and 3). Obviously, the appearance of peaks of glass transition and cold crystallization is connected with the nucleating action of GNP particles which act as nucleating agents in melt.

At GNP concentrations of 10, 15, and 20 wt% in composites, the DSC curves at the first heating demonstrated the only one pronounced melting peaks (Figure 1, curves 4, 5, and 6, Table 1).

Apparently, the absence of cold crystallization is a result of a decrease in the segmental mobility of PLA chains in the presence of a significant amount of the GNP filler.

An increase in the melting point of PLA in composites with increasing concentration of GNP indicates the formation of more perfect crystals in the presence of GNP particles, which play the role of nucleating agents (Table 1). However, it should be noted that this growth occurs only at low concentrations of GNP and then decreases with increasing concentration.

DSC data obtained under the second heating of PLA/GNP composites indicated a decrease in the melting temperatures for all PLA/GNP samples, compared with the values obtained under first heating (Figure 2; Table 1). The decrease of T_m of PLA/GNP upon the second heating is apparently explained by the formation of less perfect crystals after the first cycle of heating-cooling. The sharp decrease in the enthalpy of melting for the initial PLA at the second

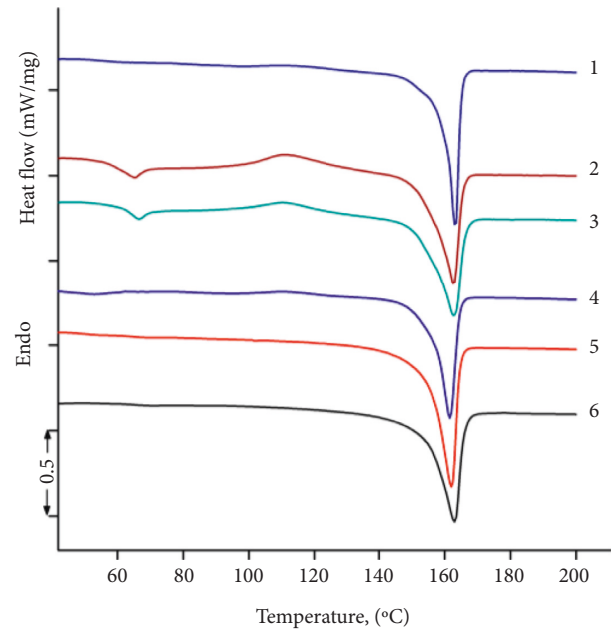


FIGURE 1: DSC curves of PLA (1) and its compositions with GNP containing 1, 1 wt%; 2, 5 wt%; 3, 10 wt%; 4, 15 wt%; 5, 20 wt% of GNP at first heating.

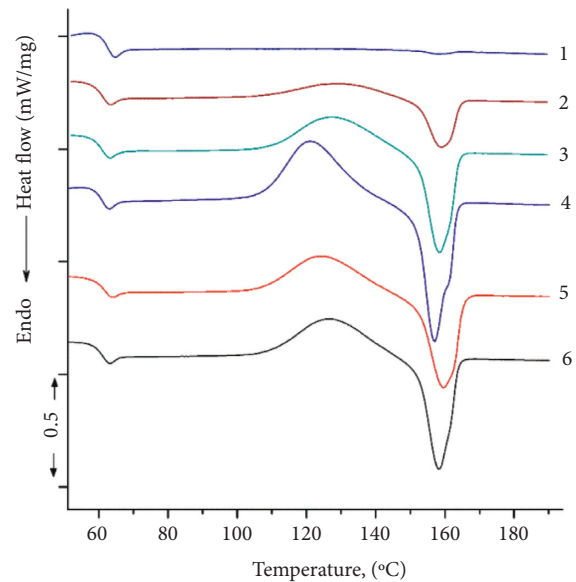


FIGURE 2: DSC curves of PLA (1) and its compositions with GNP containing 1, 1 wt%; 2, 5 wt%; 3, 10 wt%; 4, 15 wt%; 5, 20 wt% of GNP at second heating.

heating stage can be explained by its almost complete amorphization after the first heating-cooling cycle (Figure 2; Table 1).

The degree of crystallinity $\chi\%$ of initial PLA and in its composites with GNP was calculated by

TABLE 1: DSC parameters of thermal transitions observed in PLA composites.

Sample	Heating	T_g (°C)	T_{cc} (°C)	T_m (°C)	ΔH_{cc} (J/g)	ΔH_m (J/g)	Degree of crystallinity, χ (%)
PLA	First	—	—	163.2	—	-30.8	30.8
	Second	61.3	—	158	—	-0.6	0.65
PLA/GNP, 1 wt%	First	56.5	—	162.4	—	-31.8	32.2
	Second	61.6	128.6	159.0	7.1	-10.9	4.0
PLA/GNP, 5 wt%	First	64.6	111.0	162.8	5.8	-31.6	27.7
	Second	61.1	127.1	158.5	16.5	-23.4	7.8
PLA/GNP, 10 wt%	First	—	—	162	—	-31.7	32.1
	Second	62	121.3	157/162	25.5	-32.2	3.9
PLA/GNP, 15 wt%	First	—	—	162.6	—	-40.5	43.3
	Second	61.2	126.5	158/162	22.9	-26	5.5
PLA/GNP, 20 wt%	First	—	—	163.5	—	-42.1	45.0
	Second	61.7	124.5	160/163	19.6	-29.1	10.1

PLA, poly(lactic acid); GNP, graphite nanoplates.

$$\chi = \frac{\Delta H_m + \Delta H_{cc}}{\Delta H_m^{100}}, \quad (1)$$

where ΔH_m is the enthalpy of melting, ΔH_{cc} is the enthalpy of crystallization (enthalpy of “cold” crystallization), and ΔH_m^{100} is the theoretical value of the of 100% crystalline poly(L-lactide) melting enthalpy (93.6 J/g) [15].

The calculated values of the degree of crystallinity of PLA at first and second heating are 30.8 and 0.65%, respectively (Table 1), which is consistent with the data in Figure 3, and indicate the almost complete amorphization of the sample during cooling.

At the same time, as can be seen from the data in Table 1 and Figure 3, at first heating degree of crystallinity of PLA increases from 30.8% (initial PLA) to 45% in the PLA/GNP composition (80 : 20 wt%), while upon second heating, these values are only 0.65 and 10%, respectively, which is connected with amorphization of these samples under the cooling mode. The T_g values of PLA during the first and second heating of the composites change insignificantly with the increasing GNP content. Upon second heating, the broadening of the melting and glass transition peaks of PLA is observed, while the glass transition temperature slightly shifts towards lower temperatures. Under the second heating of the composites, a slight decrease of T_{cc} of PLA is observed with the increasing GNP content, which is associated with the nucleating effect of GNP (Table 1).

3.2. Thermogravimetric Analysis. The results of thermogravimetric analysis of PLA/GNP compositions are shown in Figure 4 and Table 2. Figure 4 shows the curves of weight loss (TG) and derivatives of weight loss (DTG) of the initial PLA and PLA/GNP compositions containing 1, 5, 10, and 20 wt% GNP from temperature. The obtained results are presented in Table 2, where T_{on} (onset) is the temperature of the beginning of sample decomposition, T_{max} is the temperature of the maximum decomposition rate of the sample, and $T_{5\%}$ is the temperature corresponding to 5% weight loss of the sample, determined from Figure 4. From the data shown in Figure 4 and Table 2, it is clearly seen that with the introduction of GNP in a composition, the effect of increasing

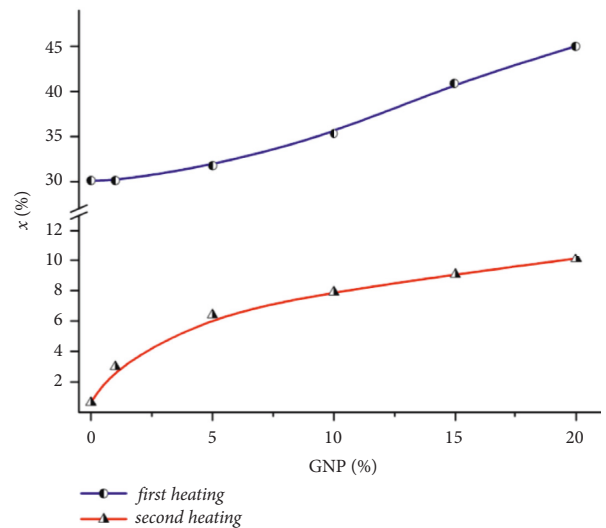


FIGURE 3: Dependence of degree of crystallinity of PLA in the compositions of PLA/GNP from content of GNP at first and second heating.

thermal stability of PLA is observed, which is expressed in a monotonic growth of all temperature indicators.

It should be noted that the maximum increase of all temperature characteristics of thermal stability in comparison with the initial PLA is observed for the PLA composition containing 20 wt% of GNP. Thus, the values of T_{on} , $T_{5\%}$, and T_{max} for the composition containing 20 wt% of GNP are greater by 24°, 30°, and 21°, respectively, compared with the initial PLA.

Figure 5 shows the curves of T_{on} , $T_{5\%}$, and T_{max} vs. the concentration of GNP in the compositions. As can be seen, the behavior of all these curves is similar.

In the literature, the effect of graphene on increasing the thermal stability of various polymers and, in particular, PLA is explained by the barrier effect, created by planar graphene particles during pyrolysis [16, 17].

It is believed that graphene particles are capable of hindering the diffusion of volatile PLA degradation products from the melt both due to the “maze effect (or tortuous path)” and due to the strong interaction of surface graphene

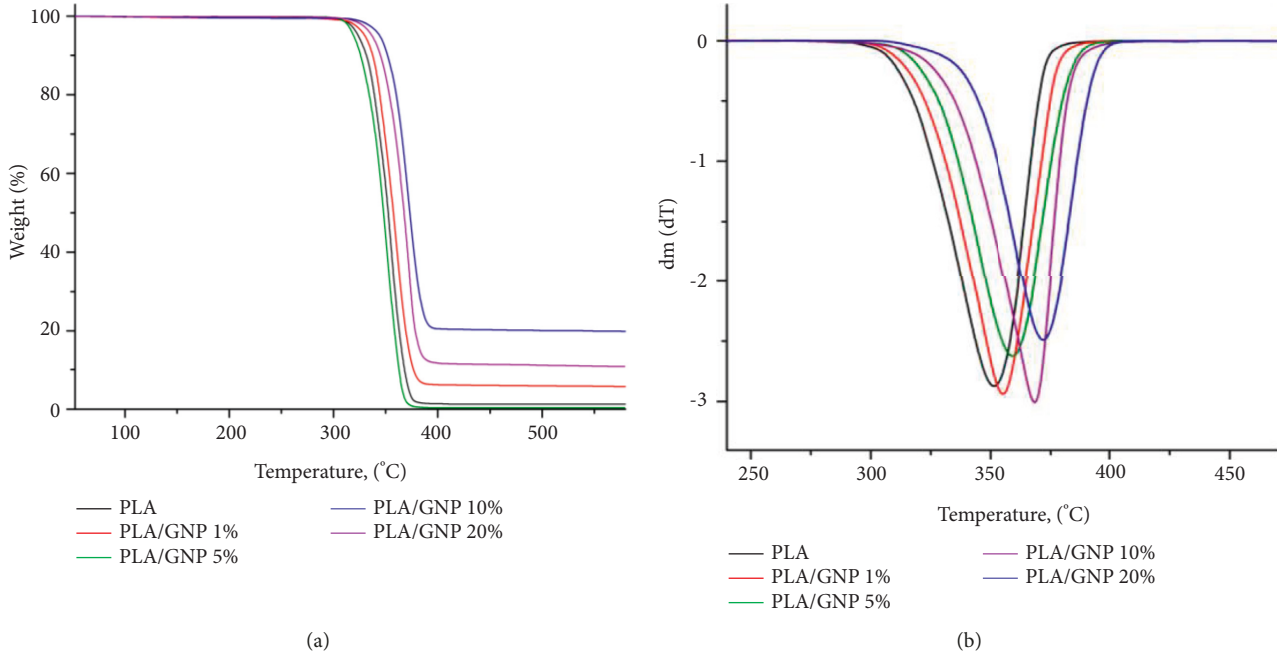


FIGURE 4: Thermograms (TG) (a) and differential thermograms (DTG) (b) of PLA and PLA/GNP composites.

TABLE 2: TGA data of PLA and PLA/GNP composites.

Content of GNP in composites (wt%)	Degradation temperature (°C)		
	T_{on}	$T_{5\%}$	T_{max}
PLA	309	313	351
1	313	323	355
5	318	329	360
10	326	336	368
20	333	343	372

PLA, poly(lactic acid); GNP, graphite nanoplates.

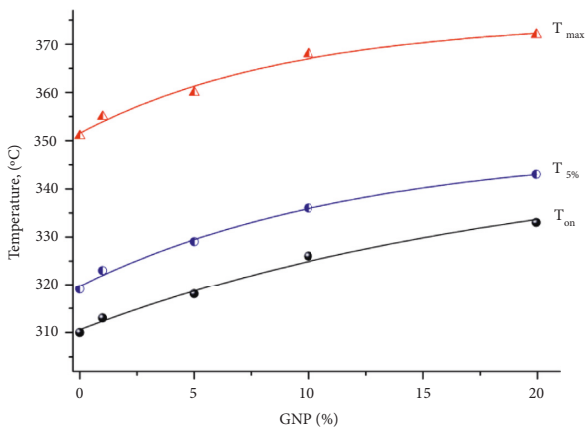


FIGURE 5: The dependences of temperatures of the T_{on} , $T_{5\%}$, and T_{max} on GNP content in compositions.

atoms and PLA polymer chains. Apparently, the interaction of the surface of graphene and PLA macrochains leads to a decrease in their segmental mobility, and as a result, the process of PLA thermal degradation slows down due to a

decrease in the rate of the intramolecular chain transfer reaction [18].

3.3. Mechanical Properties of PLA and PLA/GNP Composites.

In the general case, the deformation behavior of disperse-filled composites is determined by the properties of the polymer matrix and the filler content. Under the action of an external load, an inhomogeneous distribution of stresses develops around the fillers, which initiate local micro-mechanical deformation processes that determine the macroscopic properties of composites. The main property of the matrix is rigidity, and the important characteristics of the filler are particle size, particle size distribution, specific surface area, and particles shape. Their segregation, aggregation, and orientation determine the structure of the composite. In this case, interphase interactions lead to the formation of a rigid interphase boundary, which significantly affects the properties of the composite material [19].

Mechanical characteristics of PLA and PLA/GNP composites are given in Table 3. It is seen that the mechanical parameters of PLA are typical for glassy polymers with low elongation at break values. The addition of GNP to PLA leads to the increase in the elastic modulus, decrease in the tensile strength, and the elongation in break, which are very low for all composites. It is necessary to note that for composites, containing 20 wt% of GNP, the sharp increase in the elastic modulus (by 3 times) with simultaneous decrease in the tensile strength (2 times) and elongation in break (8 times) takes place which is the characteristic of brittle polymer systems and is clearly illustrated by the curves shown in Figure 6.

Figure 6 shows tensile diagrams in coordinates stress (σ)-relative elongation (ϵ) for PLA/GNP composites. It can

TABLE 3: Mechanical characteristics of PLA and PLA/GNP composites.

Content of GNP in composites (wt%)	E (MPa)	σ_b (MPa)	ϵ_b (%)
PLA	2700 ± 65	45.4 ± 1	4 ± 0.1
1	3220 ± 132	38.8 ± 3.5	2.0 ± 0.2
5	3550 ± 195	30.5 ± 2.7	1.5 ± 0.14
10	4466 ± 207	30.1 ± 1.7	1.0 ± 0.06
15	5088 ± 325	32.7 ± 1.4	0.9 ± 0.06
20	7735 ± 306	23.7 ± 3.5	0.5 ± 0.1

PLA, poly(lactic acid); GNP, graphite nanoplates.

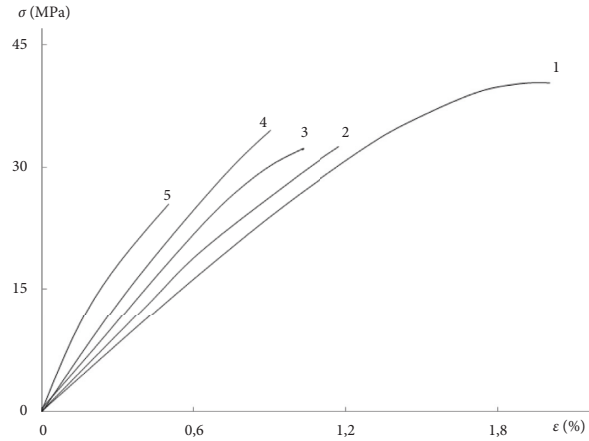


FIGURE 6: Diagrams of tensile strength (σ)–elongation in break (ϵ) of PLA/GNP at various concentrations of GNP: 1, 1 wt%; 2, 5 wt%; 3, 10 wt%; 4, 15 wt%; 5, 20 wt%.

be seen that PLA/GNP composites containing 1 wt% GNP are deformed uniformly, i.e., the stress monotonically increases with increasing deformation, while with increasing concentration of the filler, a decrease in the elongation at break ϵ_p takes place. The character of the dependence (σ)–(ϵ) remains unchanged with a further increase of the GNP content.

3.4. Electrical Properties. Figures 7(a) and 7(b) show, respectively, the dependences of the dielectric constant and conductivity on frequency at various filler concentrations, where σ_{dc} is the *dc* conductivity, σ_{ac} is the *ac* conductivity, f is the frequency, and σ is a parameter that depends on characteristics of hopping conduction [20].

$$\sigma(f) = \sigma_{dc} + \sigma_{ac} = \sigma_{dc} + Af^s, \quad (2)$$

As shown in Figure 7(a), at filler concentrations <10%, there is no plateau on the frequency dependences of conductivity, i.e., there is no bulk conduction and the percolation threshold is not reached. The bulk conduction appears at a filler concentration of 10% and is $3.5 \cdot 10^{-12} (\text{Ohm cm})^{-1}$. With further increase in the filler content, the conductivity practically does not change (Figure 8).

From the frequency dependence of σ , it can be concluded that the percolation threshold in these composites is close to 7 wt%, which is significantly lower than in the case of spherical particles of comparable density [21, 22].

The dielectric constant increases up to a concentration of 5% and then drops to values of the order of 1.5 (Figures 7(b) and 8). The decrease in the dielectric constant is apparently related to the properties of the filler. When the percolation threshold is reached, the filler forms a continuous three-dimensional cluster of contacting particles, which, with an increase in concentration due to the low compressibility of particles, does not densify, but only expands, which leads to an increase in the porosity of the composite. This manifests itself in a decrease in the dielectric constant because in this case, a certain fraction of the volume of the composite is made up of air voids with $\epsilon' = 1$.

3.5. Investigation of Composites by SEM. On Figure 9, the SEM images of PLA/GNP films containing 1% wt of GNP obtained from CH_2Cl_2 solutions are presented.

SEM images clearly evidence the PLA/GNP scaffold microporous structure of composition.

These results show that with the use of the preparation technology in solution presented in this work, a microporous structure of PLA compositions is formed. This fact was noted earlier in the works on the preparation of porous, biodegradable films, or scaffolds, which have found their application in medicine [23–26].

The films of PLA and PLA/GNP composites obtained at 55°C from CH_2Cl_2 were subjected to hot pressing on a Carver Press. The SEM images of transverse cross-sections of PLA/GNP films, prepared by hot pressing at 180°C and

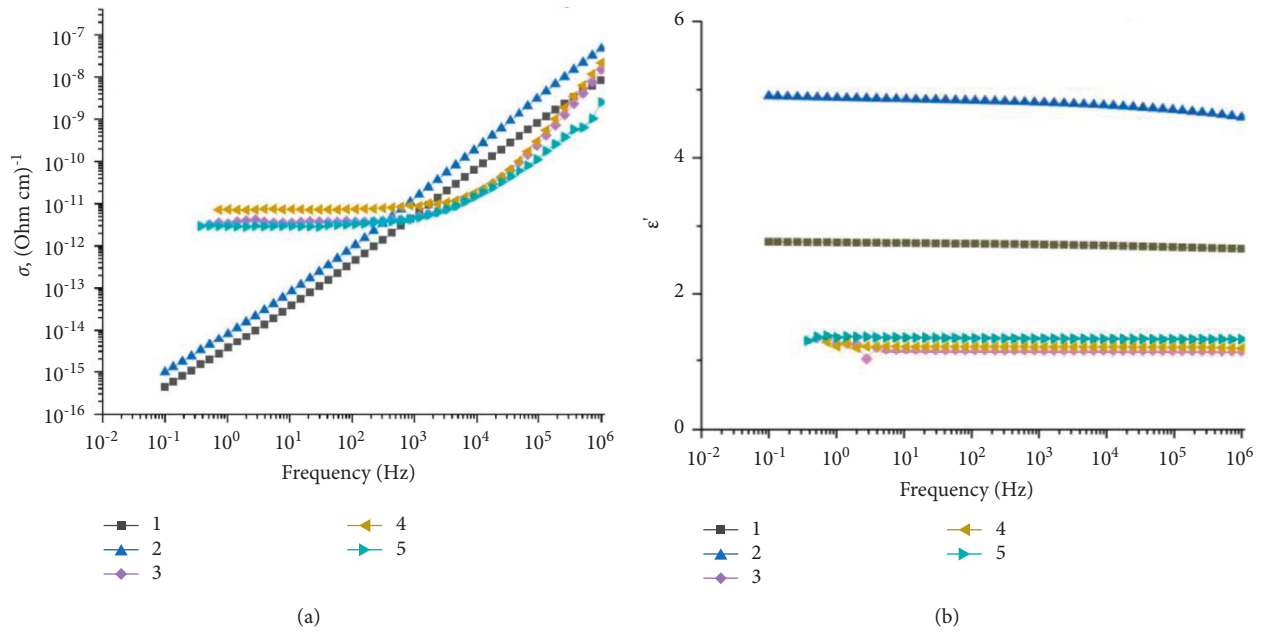


FIGURE 7: Dependences of the conductivity σ (a) and dielectric constant ϵ' (b) on frequency at various concentrations of GNP: 1, 1 wt%; 2, 5 wt%; 3, 10 wt%; 4, 15 wt%; 5, 20 wt%. For disordered three-dimensional media, which include polymer composites with conducting fillers, the frequency dependence of conductivity usually follows

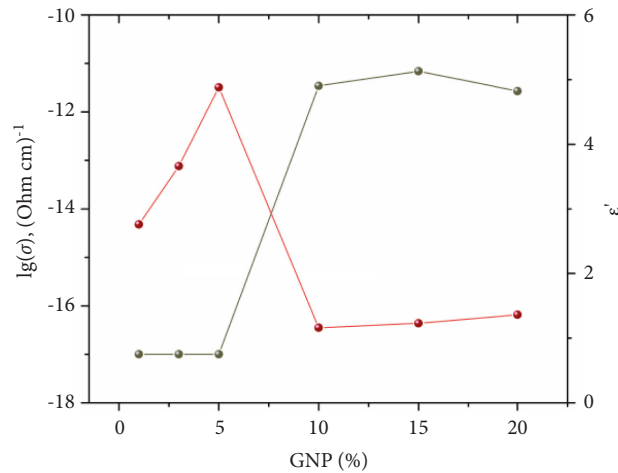


FIGURE 8: Dependences of conductivity and dielectric constant on the concentration of GNP.

containing 1, 10, and 20 wt% of GNP at different magnifications are presented in Figure 10.

Extended graphene agglomerates covered with a layer of polylactide are identified on all micrographs, which, together with the absence of cracks and cavities, indicates the cohesive destruction of systems in the polylactide phase.

It can be seen that the morphology of the fracture surface changes with an increase in the graphene concentration. The surface becomes more developed and is characterized by a larger specific area. It should be noted that the results obtained during the analysis of the phase structure of the studied systems correlate with the data of physical and mechanical studies.

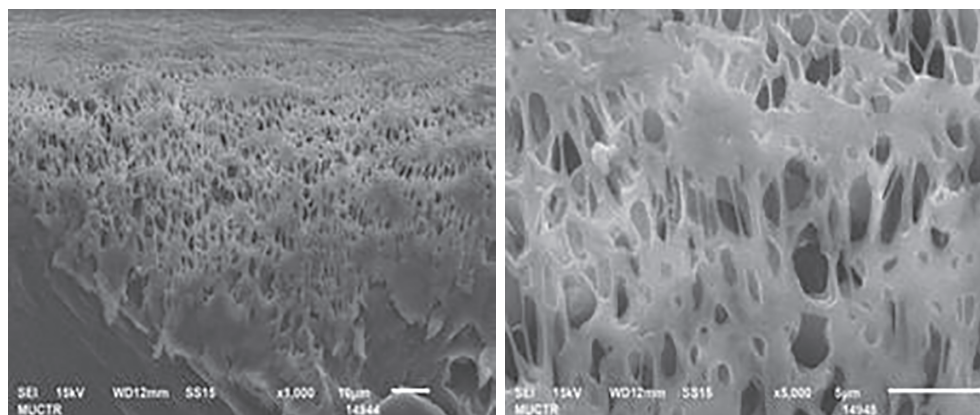


FIGURE 9: SEM images at different magnifications of PLA/GNP films containing 1 wt% of GNP ((a) x 1000; (b) x 5000).

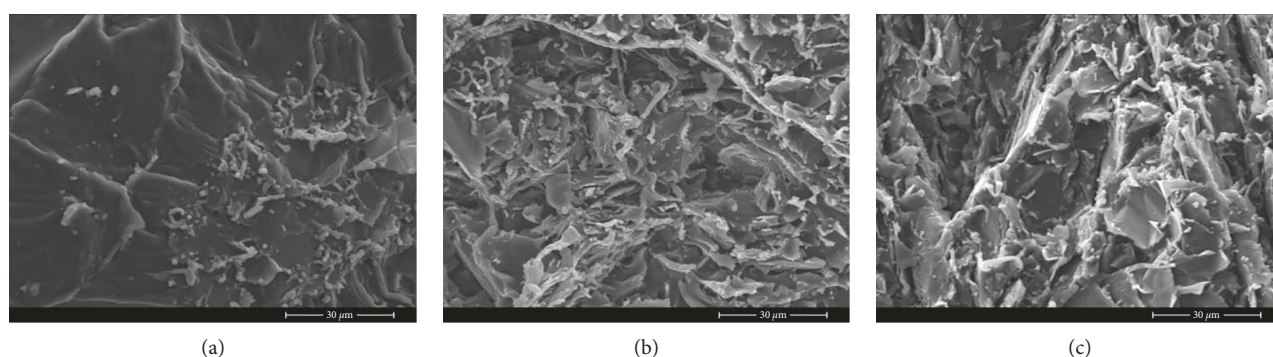


FIGURE 10: SEM images at different magnifications of cross-sections of PLA/GNP films containing 1 (a), 10 (b), and 20 (c) wt% of GNP prepared by hot pressing.

4. Conclusions

The composites of biodegradable polyester polylactide synthesized from natural renewable raw materials (lactic acid) with graphite nanoplatelets in CH_2Cl_2 solution under sonication were obtained. The thermal behavior of initial PLA and PLA/GNP film composites obtained and containing 1, 5, 10, 15, and 20 wt% of GNP was studied using DSC and TG methods. The temperatures and heats of glass transition, cold crystallization and melting and first, and secondary heating were calculated.

The mechanical characteristics of PLA and PLA/GNP composites were studied, and it was shown that the mechanical parameters of PLA composites are typical for glassy polymers with low elongation at break values. The addition of GNP to PLA leads to increase in the elastic modulus, decrease in the tensile strength, and the elongation in break, which are very low for all composites. For composites, containing 20 wt% of GNP, the sharp increase in the elastic modulus (by 3 times) with simultaneous decrease in the tensile strength (2 times) and elongation in break (8 times) takes place, which is typical for brittle polymer systems.

The study of the electrical properties of the filled composites showed that the percolation threshold in these composites is close to 7 wt%, which is significantly lower than in the case of spherical particles of comparable density.

The SEM investigation of the film composites obtained in methylene chloride showed the presence of a system of pores on the surface of the samples, which were apparently formed during the evaporation of chloroform in the process of their preparation. So, in this case, a microporous structure of PLA compositions is formed. At the same time, the SEM images of transverse cross-sections of PLA/GNP films, prepared by hot pressing at 180°C , and containing 1, 10, and 20 wt% of GNP exhibit extended graphite agglomerates covered with a layer of polylactide, which, together with the absence of cracks and cavities, indicates the cohesive destruction of systems in the polylactide phase.

Thus, the developed compositions based on PLA containing GNP have higher values of the elastic modulus E and lower values of tensile strength and elongation at break. The detected increase in the crystallinity of PLA with an increase in the GNP content contributes to an increase in the thermal stability and oxidative thermal stability of the obtained compositions, which expands the possible areas of their potential application.

Data Availability

The research data used to support the findings of this study are included within the article.

Conflicts of Interest

The authors declare that they have no conflicts of interest.

Acknowledgments

This work was supported by the Russian Science Foundation (22-23-00369).

References

- [1] S. Stankovich, D. A. Dikin, G. H. B. Dommett et al., "Graphene-based composite materials," *Nature*, vol. 13, p. 282, 2006.
- [2] B. W. Chieng, N. A. Ibrahim, W. M. Z. W. Yunus, M. Z. Hussein, Y. Y. Then, and Y. Loo, *Polymers*, vol. 6, p. 2232, 2014.
- [3] D. G. Papageorgiou, I. A. Kinloch, and R. J. Young, "Mechanical properties of graphene and graphene-based nanocomposites," *Progress in Materials Science*, vol. 90, p. 75, 2017.
- [4] A. Jiménez, M. Peltzer, and R. Ruseckaite, "Preface - Poly(lactic acid) Science and Technology," *The Royal Society of Chemistry*, vol. 34, p. 353, 2014.
- [5] O. C. Compton and S. B. T. Nguyen, *Small*, vol. 6, p. 711, 2010.
- [6] J. R. Dorgan, H. Lehermeier, and M. Mang, "Thermal and Rheological Properties of Commercial-Grade Poly(Lactic Acid)s," *Journal of Polymer Science*, vol. 8, 2000.
- [7] C. McNeill and H. A. Leiper, *Polymer Degradation and Stability*, vol. 11, p. 309, 1985.
- [8] F. D. Kopinke, M. Remmler, K. Mackenzie, M. Möder, and O. Wachsen, "Thermal decomposition of biodegradable polyesters—II. Poly(lactic acid)," *Polymer Degradation and Stability*, vol. 53, p. 329, 1996.
- [9] M. S. Södergård, "Properties of lactic acid based polymers and their correlation with composition," *Progress in Polymer Science*, vol. 6, p. 1123, 2002.
- [10] V. Taubner and R. Shishoo, *Journal of Applied Polymer Science*, vol. 79, p. 212, 2001.
- [11] V. V. Arslanov, M. A. Kalinina, E. V. Ermakova et al., *Russian Chemical Reviews*, vol. 88, p. 775, 2019.
- [12] C. Gonçalves, I. C. Gonçalves, F. D. Magalhães, and A. M. Pinto, "Poly(lactic acid) composites containing carbon," *Polymorphism*, vol. 1, 2017.
- [13] L. S. De Bortoli, R. de Farias, D. Z. Mezalira, L. M. Schabbach, and M. C. Fredel, *Materials Today Communications*, vol. 31, p. 103402, 2022.
- [14] W. Y. Lin, Y. F. Shih, C. H. Lin, C. C. Lee, and Y. H. Yu, "The preparation of multi-walled carbon nanotube/poly," *Journal of Taiwan Institution of Chemical Engineers*, vol. 44, p. 489, 2013.
- [15] E. Fischer, H. Sterzel, and G. Wegner, "Investigation of the structure of solution grown crystals of lactide copolymers by means of chemical reactions," *Colloid and Polymer Science*, vol. 980, p. 251, 1973.
- [16] R. Potts, D. R. Dreyer, C. W. Bielawski, and R. S. Ruoff, "Graphene-based polymer nanocomposites," *Polymer*, vol. 52, p. 5, 2011.
- [17] H. Kim and Y. G. Jeong, "Polylactide/exfoliated graphite nanocomposites with enhanced thermal stability, mechanical modulus, and electrical conductivity," *Journal of Polymer Science Part B: Polymer Physics*, vol. 48, p. 850, 2010.
- [18] F. D. Kopinke and K. Mackenzie, "Mechanistic aspects of the thermal degradation of poly(lactic acid) and poly(β -hydroxybutyric acid)," *Journal of Analytical and Applied Pyrolysis*, vol. 40, p. 43, 1997.
- [19] B. P. Móczó, *Encyclopedia of Polymers and Composites*, Springer, Heidelberg, Germany, 2016.
- [20] K. Jonscher, "The universa' dielectric response," *Nature*, vol. 267, p. 673, 1977.
- [21] D. W. Kim, J. H. Lim, and J. Yu, "Efficient prediction of the electrical conductivity and percolation threshold of nanocomposite containing spherical particles with three-dimensional random representative volume elements by random filler removal," *Composites Part B: Engineering*, vol. 168, p. 387, 2019.
- [22] D. E. S. De Sousa, C. H. Scuracchio, G. M. De Barra, and A. A. De Lucas, "Expanded graphite as a multifunctional filler for polymer," *Multifunc of Polym. Comp.* vol. 7, p. 245, 2015.
- [23] Y. S. Nam and T. G. Park, "Biodegradable polymeric microcellular foams by modified," *Biomaterials*, vol. 20, p. 1783, 1999.
- [24] K. L. F., M. S. S., W. R. W. Guan, "Preparation and characterization of highly porous, biodegradable polyurethane scaffolds for soft tissue applications," *Biomaterials*, vol. 26, p. 3961, 2005.
- [25] T. Moriya and Y. Ohmukai, *Journal of Membrane Science*, vol. 342, p. 307, 2009.
- [26] G. Vozzi, C. J. Flaim, F. Bianchi, A. Ahluwalia, and S. Bhatia, "Microfabricated PLGA scaffolds: a comparative study for application to tissue engineering," *Materials Science and Engineering A*, vol. 20, p. 43, 2002.